Available online at www.CivileJournal.org

Civil Engineering Journal

(E-ISSN: 2476-3055; ISSN: 2676-6957)

Vol. 9, No. 07, July, 2023

Reducing Effects of Initial Imperfection by Investment in the Orthotropic Characteristics of Laminated Composite Plate

Wisam Hamzah Mohammed [1, 2*], Svetlana Shambina [1], Haider Kadhim Ammash [2]

[1] *Peoples Friendship University of Russia (RUDN University); 6 Miklukho-Maklaya Street, Moscow, 117198, Russian Federation.*

[2] *Department of Civil Engineering, University of Al-Qadisiyah, Al Diwaniyah, Iraq.*

Received 21 January 2023; Revised 04 June 2023; Accepted 11 June 2023; Published 01 July 2023

Abstract

The target of this study is to reduce the impact of initial imperfection on the nonlinear dynamical performance of laminated composite plates by taking advantage of the orthotropic characteristics of laminated composite plates by changing carbon fiber sawing in the mass matrix and fiber orientation with different patterns and studying the effect of this optimization without and with initial imperfection (W_o) and different aspect ratios (W/L) and various boundary conditions through analyzing the load-displacement responses for plates under axial in-plane compressive loads by using the FORTRAN 94 programming language. Von-Karman's assumptions are utilized to include geometric nonlinearity for nine node isoperimetric quadrilateral components with five degrees of freedom into the structural model, which is based on first-order shear deformation theory. The Newmark's implicit time integration method and Newton-Raphson iteration concurrently are employed to solve the nonlinear governing equation in conjunction. The study proved the effectiveness of the carbon fiber's varying geometric distribution and the difference in its directions in reducing the negative effects of the initial imperfection on the large elastic-plastic displacement and critical buckling. To highlight the veracity of the results, some of them have been validated against those found in the literature review.

Keywords: Initial Imperfection; Composite Laminated Plates; Distribution Carbon Fiber; Orientation Carbon Fibers; Optimization; Dynamic Stability; Elastic-Plastic Displacement.

1. Introduction

Laminated composite plates have become the focus of many researchers since they are categorized as orthotropic (anisotropic) materials. Taking into account the fact that its constituent materials (reinforcement and a matrix) retain their chemical, physical, and mechanical properties, Stephen W. Tsai was one of the first to lay the modern foundations for understanding the behavior and resistance of these materials as well as the forms of occurrence of total and partial failure of a layer without others. Since the micromechanical approach studies the volume proportions of the constituents for the desired lamina stiffness and strength, it is found to be more appropriate for the analysis of composite materials [1]. The Tsai theory met the steady-state coordinate transformation requirements, took the interaction terms into account as separate components, took into account the difference in strengths caused by positive and negative stresses, and was specialized to take into account various material symmetries, multi-dimensional space, multi-axial stresses, and measured off-axis uniaxial. Tsai's theory was supported by the off-axis uniaxial and pure shear data's agreement with the predicted values [2]. According to failure theories based on interactive failure criteria, the lamina's failure is predicted by a single polynomial, often a quadratic equation containing all the stress components. By taking into account all of

* Corresponding author: 1042198083@pfur.ru

http://dx.doi.org/10.28991/CEJ-2023-09-07-03

the stress factors, as the failure theories in this category do, this failure criteria more closely links the theoretical values and the tests [2–5], and failure theories based on failure criteria that determine mode of failure Independent and interactive failure criteria give no information regarding the mode of failure. The failure mode and failure mode are predicted by the mode-determining failure criteria. As Hashin-Rotem (1973) points out, these failure criteria comprise different polynomial equations for each failure mode, such as fiber tension, matrix tension, fiber compression, matrix compression, and so on [6].

Based on the above concepts and the characterized ability of orthotropic materials to acquisition improvements in their hybrid properties and possibility represented the initial imperfection as a percentage of the total thickness of the laminated composite plate, was adopted the effectiveness the variable orientation of fiber for orthogonal layers ,changing the distribution pattern for carbon fibers and figuration of fibers as basic paths in making improvements in this type of plats and reducing the negativism effects of many deficiencies and manufacturing deformations, and gave flexibility in developing design requirements, the variable orientation of fiber for orthogonal layers was a first pathway the researchers took since 1973 by Adams and Bacon and proved the effectiveness of this optimizations on the dynamic performances of laminated composite plate [7]. In 1990, Brown introduced the concept of a variable fiber distribution in the mass matrix for the composite laminate by Leissa & Martine [8].

The first to prove the effectiveness of changing the figuration of straight fibers into a regular geometric wave on increasing the dent resistance of composite panels was Pandey in 1999 [9]. The researchers worked on developing the theories, foundations, and previously conducted research studies by achieving and proving relationships between the improvements associated with the direction, distribution, and figuration of the fibers, either alone or in combination, in the interfacial (orthotropic) structural of the laminated composite plates and their dynamic performance in their linear and nonlinear behavior with the variety of loading conditions, boundary conditions, and temperatures, the various design requirements, such as the holes, the variation in thickness, the various aspect ratios (W/L), etc. Important studies related to the main subject of this study (reducing the negativism effects of initial imperfection by resorting to optimizations in the direction and distribution of fibers) are highlighted in the literature of this study, which showed that this study is unique in its analyzed approach, as it will follow an innovative inductive pattern that enables specialists in the manufacture of composite panels to invest in the orthotropic mechanical properties of laminated composite plate to get the best dynamic performance without having to change the geometric features such as thickness, dimensions, aspect ratio, or slenderness ratio.

2. Literature Review

Many research paths have been taken in analyzing the imperfect laminated composite plates, linearly, non-linearly, statically, and dynamically, that often occur during the industry stages because of the employment of heat, cooling, hammering, and pressing during their manufacture or installation in structures. Studies that focused on studying the initial deficiency and its effects on the bearing capacity of the panels under different conditions and multiple engineering and structural parameters The oldest of the studies that have been published was by Williams & Walker (1976), discussed the relationship of the mesh size in relation to the first - order finite difference approximation of the derivatives in the Van-Karman large defluxion differential equation to determining the real effect of the initial deformed resulting from the dynamic relaxation part in the plastic limits and proved that the mesh size (8 × 8) was most accurate in extracting the satisfactory value of the collapse stresses of the imperfect plate, this study was not concerned with the laminated characteristics of the orthotropic (anisotropic) laminated composite plates and the behavior of the anisotropic materials [10].

Yang et al. (2006) study the effect of the various possible initial geometrical imperfections, such as sine type, local type, and global type imperfections, and the effects of decrease parameters, half-wave number, amplitude, and location on the post-torsion response of the plates with a uniform temperature change. Although this study deals with the study of a different plate from the current study, it shows clearly the effect of the initial imperfection on plates and proves the excitement susceptibility of shear deformable functionally graded plates post-buckling for initial geometrical imperfections by the imperfection function that takes the form of the product of trigonometric and hyperbolic functions. This study is an important reference to show the outstanding performance of the laminated composite plates compared with the deformable functionally graded plates for the same percentage of initial imperfection and under the same conditions of temperature, boundary conditions, aspect ratio, and slenderness ratio [11].

Feddal et al. (2018) conducted a non-linear analysis of a laminated composite plate with eight reinforced layers of carbon fibers fixed at all its edges. Are studied with three values of initial imperfection (2, 4, and 6 mm) by the ABAQUS program to investigate the effect of fiber orientations in successive layers on the stiffened deficient plate. The study is worth mentioning, but it didn't include a value of the buckling strength of the composite plate without the studied added geometric properties (stiffness, imperfection, and fiber orientation) to evaluate the impact clearly [12]. The initial

imperfections study presented by Ghannadpour & Mehrparvar (2019) was characterized by the fact that it studied the geometrically nonlinear behavior of relatively thick composite laminates with two weaknesses in the study model at the same time, containing square and rectangular cutouts as initial geometric imperfections. The effects of cutout size, shape, and the presence of initial geometric imperfection on plates under uniaxial in-plane compressive load are also studied [13]. Al-Ramahee & Abodi (2020) studied the effect of changing the fiber distribution on the dynamic behavior with a large damping ratio of the laminated composite plate. They studied the effect of the initial imperfection by changing the damping ratio on the dynamic behavior of the laminated composite plate with a variable distribution of fibers according to the Lies-Martin equations, but they did not discuss the effect of the initial deficiency on the behavior of the plate [14].

In the study of Mondal & Ramachandr (2020), the non-linear dynamic pulse torsion of a defective composite panel with numerically integrated discharge that represents the openings in the laminated composite plate as an imperfection was analyzed. This study's results were chosen to verify the accuracy of the current results and the reliability of the programmed and calculated responses of the disassembled plates to different discharge ratios at different layer interfaces using the Tsai-Wu quadratic reaction criterion and show the effect of pulse load type (sinusoidal, exponential, and rectangular) and plate boundary condition on the trauma spectrum [15]. Cetkovic (2022) This study proved the effects of different geometric parameters (aspect ratio, slenderness ratio, lamination scheme, and boundary conditions) on the critical buckling temperature of the imperfect laminated composite plate by analyzing the thermal shrinkage of the laminated composite plate with initial geometrical imperfection using the MATLAB program and based on the finite element theory and Redi's generalized layer theory (GLPT) [16]. Recently, the most interesting path pursued by the researchers in search of optimization and minimizing the effect of defects in the laminated composite plate affecting their interfacial structure has been the sawing of the fibers in regular geometrical waves.

In Thor et al. (2022), the compatibility of the numerical simulation with the experimental data was distinguished in this study, as were many parameters studied in the theoretical aspect, such as amplitude, wavelength, and plate thickness. The study showed that the failure changed from discharge to crosslinked shear strip formation as sheet thickness increased and that wavelength had minor effects compared to sheet amplitude and thickness [17]. Most of the literature mentioned in this study and others focused only on the side effects of the initial imperfection on the critical buckling, large elastic-plastic displacement, or reducing the bearing capacity in general and did not address the improvements that can be made in the structural structure of the laminated composite plates for reducing the imperfection effects, depending on the characteristics of the orthotropic materials that endow these materials with a high susceptibility to optimizations. Therefore, the current study corrected this through the study of the initial imperfection with the presence of some improvements, such as changing the distribution of fibers and changing their direction, to reduce the effect of the initial deficiency on the resistance and behavior of the imperfect plates.

3. Theoretical Formulation

Consider a laminated composite plate that has dimensions of length a, breadth b, and thickness h and is subjected to a compressive force that is applied in a single direction and pulses. Orthotropic material with a material axis parallel to the edges is used to create the layers of the composite laminate. Only at the zone of delamination are sub laminates separated.

3.1. Layer Wise Plate Theory

The laminated composite plate is modeled using Reddy's Generalized Laminated Plate Theory (GLPT) [18]. Here, it is assumed that there is a geometric defect in the form of transverse displacement w. In an n-layered plate with delamination at ND number of layer interfaces, the total displacement field (u1, u2, u3) along global coordinate directions is represented as [15],

$$u_1(x,y,z) = u(x,y) + \sum_{I=1}^{N} vI\,(x,y)\emptyset^I\,(z) + \sum_{I=1}^{ND} U^I(x,y)H^I\,(z) \quad (1)$$

$$u_2(x,y,z) = v(x,y) + \sum_{I=1}^{N} vI\,(x,y)\emptyset^I\,(z) + \sum_{I=1}^{ND} V^I(x,y)H^I\,(z) \quad (2)$$

$$u_3(x,y,z) = w^*(x,y) + w(x,y) + \sum_{I=1}^{ND} W^I(x,y)H^I\,(z) \quad (3)$$

N is the number of arithmetic layers, which is equal to (n + 1). Along the global coordinate axes, the middle plane displacement components are represented by the letters (*u, v, and w*). (u^I, v^I, *0*) stands for the displacements at the Ith numerical layer relative to the central plane. The linear Lagrange interpolated function φ^I, which was built by the nodes at layer interfaces, interpolates variations of in-plane displacements along the transverse direction. B-spline functions interpolate the in-plane variation of in-plane and out-of-plane displacements (Figure 1). Delamination is represented as displacement components (U^I, V^I *and WI*) using the Heaviside step method and is modeled as a jump discontinuity in the displacement field.

Function H^I (Equation 4). Here, superscript I denotes the I[th] numerical layer:

$$H^I(Z) = \begin{cases} 1 & for\ z \geq z_I \\ 2 & for\ z < z_I \end{cases} \quad (4)$$

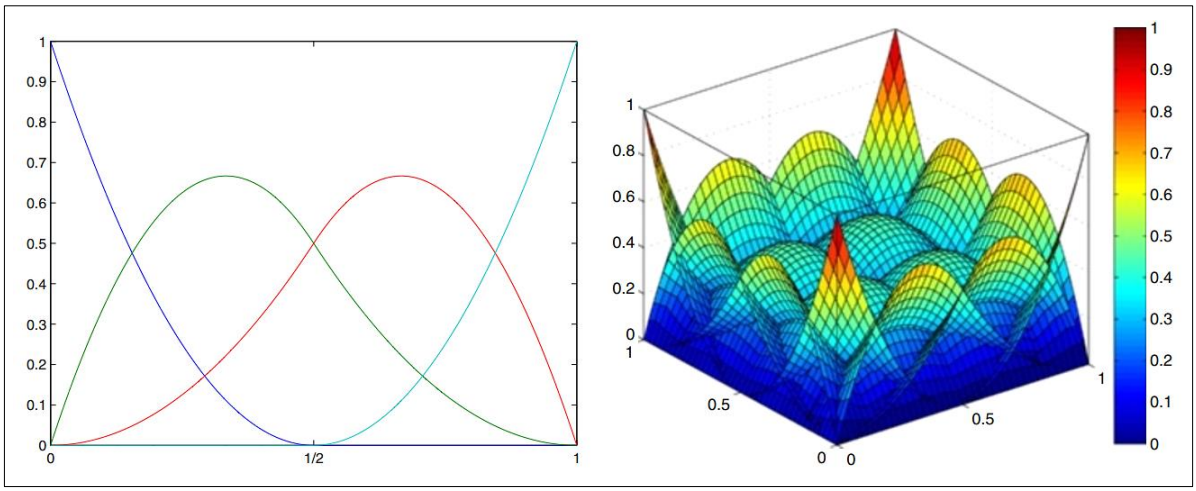

Figure 1. 1D and 2D cubic B-spline basis functions [19]

Using von Kármán strain-displacement equations as shown in Equations 5 to 11 for linear components and Equation 12 for nonlinear components, the current issue assumes minor stresses with relatively substantial displacement.

$$\epsilon^I_{xx} = u_{1,x} = u_{,x} + \sum_{I=1}^{N} u^I_{,x}\,\phi^I + \sum_{I=1}^{ND} U^I_{,x}\,H^I\,(z) \quad (5)$$

$$\epsilon^I_{yy=}u2,y = v,y + \sum_{I=1}^{N} v^I_{,y}\,\phi^I + \sum_{I=1}^{ND} V^I_{,y}\,H^I\,(z) \quad (6)$$

$$\gamma^I_{xy} = u_{1,y} + u_{2,x} = u_{,y} + v_{,x},x + \sum_{I=1}^{N}(u^I_{,y} + v^I_{,x})\,\phi^I + \sum_{I=1}^{ND}(U^I_{,y} + V^I_{,x})\,H^I \quad (7)$$

$$\gamma^I_{xz} = u_{1,z} + u_{3,x} = w_{,x} + \sum_{I=1}^{N} u^I\,\phi^I_{,z} + \sum_{I=1}^{ND} W^I_{,x}\,H^I \quad (8)$$

$$\gamma^I_{xz} = u_{2,z} + u_{3,y} = w_{,y} + \sum_{I=1}^{N} v^I\,\phi^I_{,z} + \sum_{I=1}^{ND} W^I_{,y}\,H^I \quad (9)$$

$$\epsilon^{NL}_{xx} = \frac{1}{2}\,(w_{,x})^2 w_{,x}w^*_{,x} + \sum_{I=1}^{ND}(w_{,x}W^I_{,X}H^I + w^*_{,x}W^I_{,x}H^I) + \frac{1}{2}\sum_{I=1}^{ND}\ \sum_{I=1}^{ND} W^I_{,x}W^I_{,x}H^IH^J \quad (10)$$

$$\epsilon^{NL}_{yy} = \frac{1}{2}\,(w_{,y})^2 w_{,y}w^*_{,y} + \sum_{I=1}^{ND}(w_{,y}W^I_{,Y}H^I + w^*_{,y}W^I_{,y}H^I) + \frac{1}{2}\sum_{I=1}^{ND}\ \sum_{I=1}^{ND} W^I_{,x}W^I_{,x}H^IH^J \quad (11)$$

$$\gamma^{NL}_{xy} = w_{,x}w_{,y} + w_{,y}w^*_{,x} + w_{,x}w^*_{,y} + \sum_{I=1}^{ND}(w_{,x}W^I_{,y}\,H^I + w_{,y}W^I_{,x}\,H^I) + \sum_{I=1}^{ND}\ w^*_{,x}W^I_{,y}\,H^I + w^*_{,x}W^I_{,x}\,H^I) + \sum_{I=1}^{ND}\ \sum_{I=1}^{ND} W^I_{,x}W^J_{,y}H^IH^J \quad (12)$$

There are no strain components in the plate's initial imperfection. Therefore, the initial imperfection-related strain components (Equation 13) are subtracted from the total strain

$$\epsilon^*_{xx} = \frac{1}{2}\,(w^*_{,x})^2; \epsilon^*_{yy} = \frac{1}{2}(w^*_{,y})^2; \epsilon^*_{xy} = w^*_{,x}w^*_{,y}; \epsilon^*_{xz} = w^*_{,x}; \epsilon^*_{,y} = w^*_{,y} \quad (13)$$

The global stresses $\{\sigma\}^k = \{\sigma_{xx}, \sigma_{yy}, \tau_{xy}, \tau_{xz}, \tau_{yz}y\}^{k^T}$ in the kth lamina are related to global strain components $\{\varepsilon\}^k = \{\varepsilon_{xx}, \varepsilon_{yyy}, \gamma_{xy}, \gamma_{xz}, \gamma_{yz}\}^{k^T}$ using the transformed constitutive matrix Q^k along global coordinate direction as,

$$\sigma^K = Q^K\,\varepsilon^K \quad (14)$$

The governing equilibrium equations of the imperfect plate subjected to pulse loading is derived from the Hamilton's principle and is stated as,

$$\delta \int_{t_1}^{t_2}(T-\Pi)dt = 0 \tag{15}$$

where, δT is the first variation of kinetic energy and $\delta\Pi$ is the first vatiation of total potential energy (U − V). The first variation of total strain energy (δU) is divided into linear δU_{NL} (Equation 16) and nonlinear δUNL (Equation 17) parts with the stress resultants written as in Equation 12.

$$\begin{aligned}\delta U^{L} = \int_{\Omega}\big[&N_{xx}\delta u_{,x}, + N_{yy}\delta v_{,y} + N_{xy}\big(\delta u_{,y} + \delta v_{,x}\big) + Q_x x\delta w_{,x}, + Q_y\delta w_{,y} + \sum_{I=1}^{N}\big(N_{xx}^{I}\delta u_{,x}^{I} + N_{yy}^{I}\delta v_{,y}^{I} + \\ &N_{xy}^{I}\big(\delta u_{,y}^{I} + \delta v_{,x}^{I}\big) + Q_x^{I}\delta u^{I} + Q_y^{I}\delta v^{I}\big) + \sum_{I=1}^{ND}\big(\bar{N}_{xx}^{I}\delta U_{,x}^{I} + \bar{N}_{yy}^{I}\delta V_{,y}^{I} + \bar{N}_{xy}^{I}\big(\delta U_{,y}^{I} + \delta V_{,x}^{I}\big) + \bar{Q}_x^{I}\delta W_{,x}^{I} + \\ &\bar{Q}_y^{I}\delta W_{,y}^{I}\big]d\Omega\end{aligned} \tag{16}$$

$$\begin{aligned}\boldsymbol{\delta U^{NL}} = \int_{\Omega}[\,&N_{xx}w_{,x}\delta w_{,x} + N_{yy}w_{,y}\delta w_{,y} + N_{xy}\big(w_{,y}\delta w_{,y} + w_{,x}\delta w_{,y}\big) + N_{xx}w_{,x}^{*}\delta w_{,x} + N_{yy}w_{,x}^{*}\delta w_{,y} + N_{xy}\big(w_{,x}^{*}\delta w_{,y} + \\ &w_{,y}^{*}\delta w_{,x}\big) + \bar{N}_{xx}^{I}(\delta w_{,x}\textstyle\sum_{I=1}^{ND}W_{,x}^{I} + w_{,x}\sum_{I=1}^{ND}\delta W_{,x}^{I} + \bar{N}_{yy}^{I}(\delta w_{,y}\sum_{I=1}^{ND}W_{,y}^{I} + w_{,y}^{*}\sum_{I=1}^{ND}\delta W_{,y}^{I}) + \bar{N}_{xx}^{I}\delta w_{,x}^{*}\sum_{I=1}^{ND}W_{,x}^{I} + \\ &\bar{N}_{yy}^{I}\delta w_{,y}^{*}\sum_{I=1}^{ND}W_{,y}^{I} + \bar{N}_{xy}^{I}\big(\delta w_{,x}^{*}\sum_{I=1}^{ND}W_{,y}^{I} + w_{,y}^{*}\sum_{I=1}^{ND}\delta w_{,y}^{I}\big) + \bar{N}_{xy}^{I}\big(\delta w_{,x}\sum_{I=1}^{ND}\delta W_{,y}^{I} + w_{,x}\sum_{I=1}^{ND}\delta W_{,x}^{I} + w_{,y}\sum_{I=1}^{ND}W_{,X}^{I} + \\ &w_{,y}\sum_{I=1}^{ND}\delta W_{,X}^{I}\big) + \bar{N}_{xx}^{IJ}\sum_{IJ=1}^{ND}\tfrac{1}{2}\big(W_{,x}^{J}\delta W_{,x}^{I} + W_{,x}^{I}\,\delta W_{,x}^{J}\big) + \bar{N}_{yy}^{IJ}\sum_{IJ=1}^{ND}\tfrac{1}{2}\big(W_{,y}^{J}\delta W_{,y}^{I} + W_{,y}^{I}\delta W_{,y}^{J}\big) + \bar{N}_{xy}^{IJ}\sum_{IJ=1}^{ND}(W_{,y}^{J}\delta W_{,x}^{I} + \\ &W_{,x}^{I}\delta W_{,y}^{J})\,]d\Omega\end{aligned} \tag{17}$$

The force and moment resultants used in energy expressions are computed as:

$$(\mathrm{N}_x,\ \mathrm{N}_y,\ \mathrm{N}_{xy},\ \mathrm{Q}_x,\ \mathrm{Q}_y\ ) = \sum_{K=1}^{N}\int_{Z_k}^{Z_{k+1}}(\sigma_x,\sigma_y,\tau_{xy},\tau_{xz},\ \tau_{yz})^{k}\,\mathrm{dz} \tag{18}$$

$$(\mathrm{N}_{xx}^{I},\ \mathrm{N}_{yy}^{I},\mathrm{N}_{xy}{}_{xy}^{I}\ ) = \sum_{K=1}^{N}\int_{Z_k}^{Z_{k+1}}(\sigma_{xx},\sigma_{yy},\tau_{xy})^{k}\,\emptyset^{I}\mathrm{dz} \tag{19}$$

$$\big(Q_x^{I},Q_y^{I}\big) = \sum_{k=1}^{N}\int_{z_k}^{z_{k+1}}(\tau_{xz}\,,\tau_{yz}\,)^{k}\,\emptyset_{,z}^{I}\,dz \tag{20}$$

$$(\bar{\mathrm{N}}_{xx}^{I},\ \bar{\mathrm{N}}_{yy}^{I},\ \bar{\mathrm{N}}_{xy}^{I},\ \bar{\mathrm{Q}}_{x}^{I},\ \bar{\mathrm{Q}}_{y}^{I}\ ) = \sum_{K=1}^{N}\int_{Z_k}^{Z_{k+1}}(\sigma_x,\sigma_y,\tau_{xy},\tau_{xz},\ \tau_{yz})^{k}\,H^{I}\mathrm{dz} \tag{21}$$

$$(\bar{\mathrm{N}}_{xx}^{IJ},\ \bar{\mathrm{N}}_{yy}^{IJ},\ \bar{\mathrm{N}}_{xy}^{IJ},\ \bar{\mathrm{Q}}_{x}^{IJ},\ \bar{\mathrm{Q}}_{y}^{IJ}\ ) = \sum_{K=1}^{N}\int_{Z_k}^{Z_{k+1}}(\sigma_x,\sigma_y,\tau_{xy},\tau_{xz},\ \tau_{yz})^{k}\,H^{I}H^{J}\mathrm{dz} \tag{22}$$

Considering consistent mass, the kinetic energy T is expressed as in Equation 15 with the inertia terms expressed as in Equation 16:

$$\begin{aligned}\delta T = \int_{\Omega}\big[&\mathrm{I}^{\mathrm{O}}(\ddot{\mathrm{u}}\delta\mathrm{u} + \ddot{\mathrm{v}}\delta\mathrm{v} + \ddot{\mathrm{w}}\delta\mathrm{w}) + \sum_{\mathrm{I}=1}^{\mathrm{N}}\mathrm{I}^{\mathrm{I}}(\ddot{\mathrm{u}}^{\mathrm{I}}\delta\mathrm{u} + \ddot{\mathrm{v}}^{\mathrm{I}}\delta\mathrm{v} + \ddot{\mathrm{u}}^{\mathrm{I}}\delta\mathrm{u}^{\mathrm{I}} + \ddot{\mathrm{v}}\delta\mathrm{v}^{\mathrm{I}} + \sum_{\mathrm{I}=1}^{\mathrm{N}}\sum_{\mathrm{J}=1}^{\mathrm{N}}\mathrm{I}^{\mathrm{IJ}}(\ddot{\mathrm{u}}^{\mathrm{I}}\delta\mathrm{u}^{\mathrm{J}} + \ddot{\mathrm{v}}^{\mathrm{I}}\,\delta\mathrm{v}^{\mathrm{J}} + \\ &\sum_{\mathrm{I}=1}^{\mathrm{ND}}\bar{\mathrm{I}}^{\mathrm{I}}\big(\ddot{\mathrm{U}}\delta\mathrm{u} + \ddot{\mathrm{V}}^{\mathrm{I}}\delta\mathrm{v} + \ddot{\mathrm{W}}^{\mathrm{I}}\delta\mathrm{w} + \ddot{\mathrm{u}}\delta\mathrm{U}^{\mathrm{I}} + \ddot{\mathrm{v}}\delta\mathrm{V}^{\mathrm{I}} + \ddot{\mathrm{w}}\delta\mathrm{W}^{\mathrm{I}}\big) + \sum_{\mathrm{I}=1}^{\mathrm{N}}\sum_{\mathrm{J}=1}^{\mathrm{ND}}\bar{\mathrm{I}}^{\mathrm{IJ}}(\ddot{\mathrm{u}}^{\mathrm{I}}\delta\mathrm{U}^{\mathrm{J}} + \ddot{\mathrm{v}}^{\mathrm{J}}\delta\mathrm{V}^{\mathrm{I}} + \ddot{\mathrm{U}}^{\mathrm{J}}\delta\mathrm{u}^{\mathrm{I}} + \ddot{\mathrm{V}}^{\mathrm{J}}\delta\mathrm{v}^{\mathrm{I}}) + \\ &\sum_{\mathrm{I}=1}^{\mathrm{ND}}\sum_{\mathrm{J}=1}^{\mathrm{ND}}\check{\mathrm{I}}^{\mathrm{IJ}}(\ddot{\mathrm{U}}^{\mathrm{I}}\delta\mathrm{U}^{\mathrm{J}} + \ddot{\mathrm{V}}^{\mathrm{I}}\delta\mathrm{V}^{\mathrm{J}} + \ddot{\mathrm{W}}^{\mathrm{I}}\delta\mathrm{W}^{\mathrm{J}})\big]d\Omega\end{aligned} \tag{23}$$

$$(I^{0},I^{I},I^{IJ},\bar{I}^{I}\,,\ \bar{I}^{IJ}\,,\tilde{I}^{IJ}\,)^{T}\sum_{k=1}^{N}\int_{z_k}^{z_{k+1}}\rho^{k}\ [1,\phi^{I},\phi^{I}\ \phi^{J}J\,,H^{I},\phi^{I}H^{J},H^{I}H^{J}]^{k}\,\mathrm{dz} \tag{24}$$

where, ρ is the mass density of the material. In the present analysis, the plate is subjected to uniform in-plane compressive forces, expressed in the form of stresses σ_{xx}^{0} , $\sigma_{yy}^{0}$and $\tau_{xy}^{0}$with the stress resultants as:

$$(N_{xx}^{0},N_{yy}^{0},N_{xy}^{0}) = \sum_{k=1}^{N}\int_{z_k}^{z_{k+1}}\big(\sigma_{xx}^{0},\sigma_{yy}^{0}\,,\ \tau_{xy}^{0}\big)^{k}\ dz \tag{25}$$

The first variation of work done by the applied loading is expressed as:

$$\delta V = [N_{xx}^{0}w_{,x},\delta w_{,x} + N_{yy}^{0}w_{,y}, + N_{xy}^{0}(w_{,x}\delta w_{,y} + w_{,y}\delta w_{,x}\,)]d\Omega \tag{26}$$

In the present analysis in-plane force in x direction only is acting on the plate and hence all other force components are neglected i.e. $N_{yy}^{0} = N_{xy}^{0} = 0$.

4. Materials and Methods

Table 1 is shown the one hundred cases were analyzed non-linearity dynamically of a laminated composite plates (h=0.01m) formed four layers thin steel plate fastened by the epoxy matrix reinforced fibers carbon (E_f = 413.68 [GPa], E_m = 4.3 [GPa], G_f = 172.36 [GPa], G_m = 1.277 [GPa], v_f = 0.2, and v_m = 0.35) are subjected to 800 KN uniform in-plane-plane compression load with X-axis direction in a time step *(Δt)* of 0.0001[sec],were programed Newmark integration method with α=1/2, and β=1/4 by the FENSDAAP computer program is coded in FORTRAN 94 language, which its structure chart is shown in Figure 2 , in order to study the effect of initial imperfection in center on the large elastic-plastic displacement of laminated composite plate ,where four cases of initial imperfection *(wo/h)* (0,0,0.25,0.5,1) with a unified distribution fibers, unified direction fibers , three aspect ratio (0.5, 1 and 2) when the boundary condition is SSSS, and three boundary conditions (SSSS (all edges simply supported, SCSC (two edges in load direction clamped and other two edges simply supported) and CCCC (all edges clamped)) when the aspect ratio is 1, as well as, the same cases of initial imperfection with the same aspect ratios and boundary conditions above were analyzed after modification to the model's inter structure through variable distribution of carbon fibers based on the equations of Leissa & Martine (Equations 2-2 and 3-3) as shown in Table 1 with an unified fiber direction and then a symmetrical orientation (0, 90, -90, 0) Figure 2 describes the isoperimetric nine-node Lagrangian elements, which are divided into a 22 element mesh and have five degrees of freedom per node ($w, \theta x, \theta y, \theta x^*, \theta y^*$) Little membrane stress in the transverse direction may occur because the boundary condition of the plate is simple support and the in-plane displacements of the unloaded edges are unrestrained. The thickness of the quarter plate is separated into four layers and modeled using a (2×2) mesh.

Table 1. Showing the analyzed cases

Initial imperfection (wo/h)	Aspect ratio(a/b)	Boundary condition	Fibers distribution	Orientation distribution
0.00	0.5	SSSS	Unified	Unified direction θ (0,0,0,0)
0.25				
0.5	1.0	SCSC	Equation 2-2	Unsymmetrical θ (0,90,0,90)
1.0	2.0	CCCC	Equation 3-3	

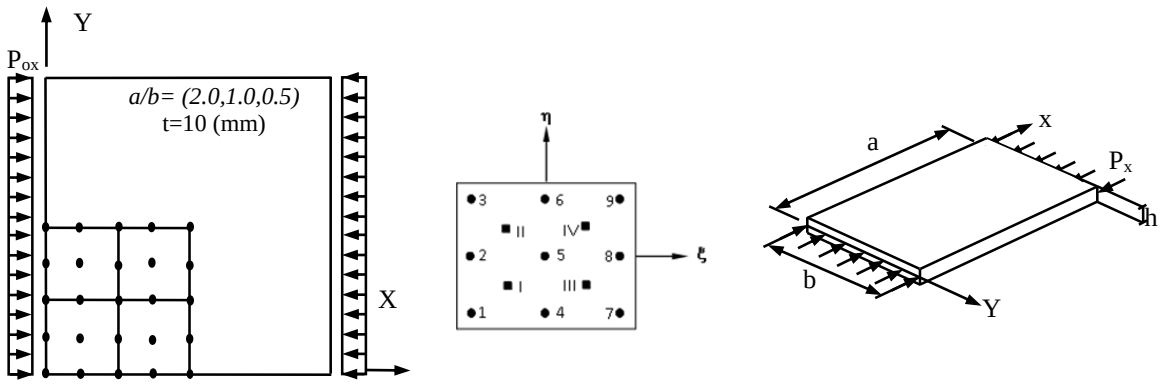

Figure 2. Description at the modeling [20]

Table 2. Leissa and Martine's equations [9]

Equation n-p (n: equation's number, p: equation's exponent)	$V_f(x)$	Volume fraction of fiber (%)	
		$V_{f\,max.}$	$V_{f\,av.}$
Equation 1-1	$[\frac{4}{L}X - \frac{4}{L^2}X^2]$	100	66.67
Equation 2-2	$[\frac{4}{L}X - \frac{4}{L^2}X^2]^2$	100	53.34
Equation 3-3	$[\frac{4}{L}X - \frac{4}{L^2}X^2]^3$	100	45.7
Equation 4-1	$\frac{1}{2}+[\frac{1}{L}X - \frac{1}{L^2}X^2]$	75	66.67
Equation 5-2	$\frac{1}{2}+[\frac{1}{L}X - \frac{1}{L^2}X^2]^2$	75	63.34

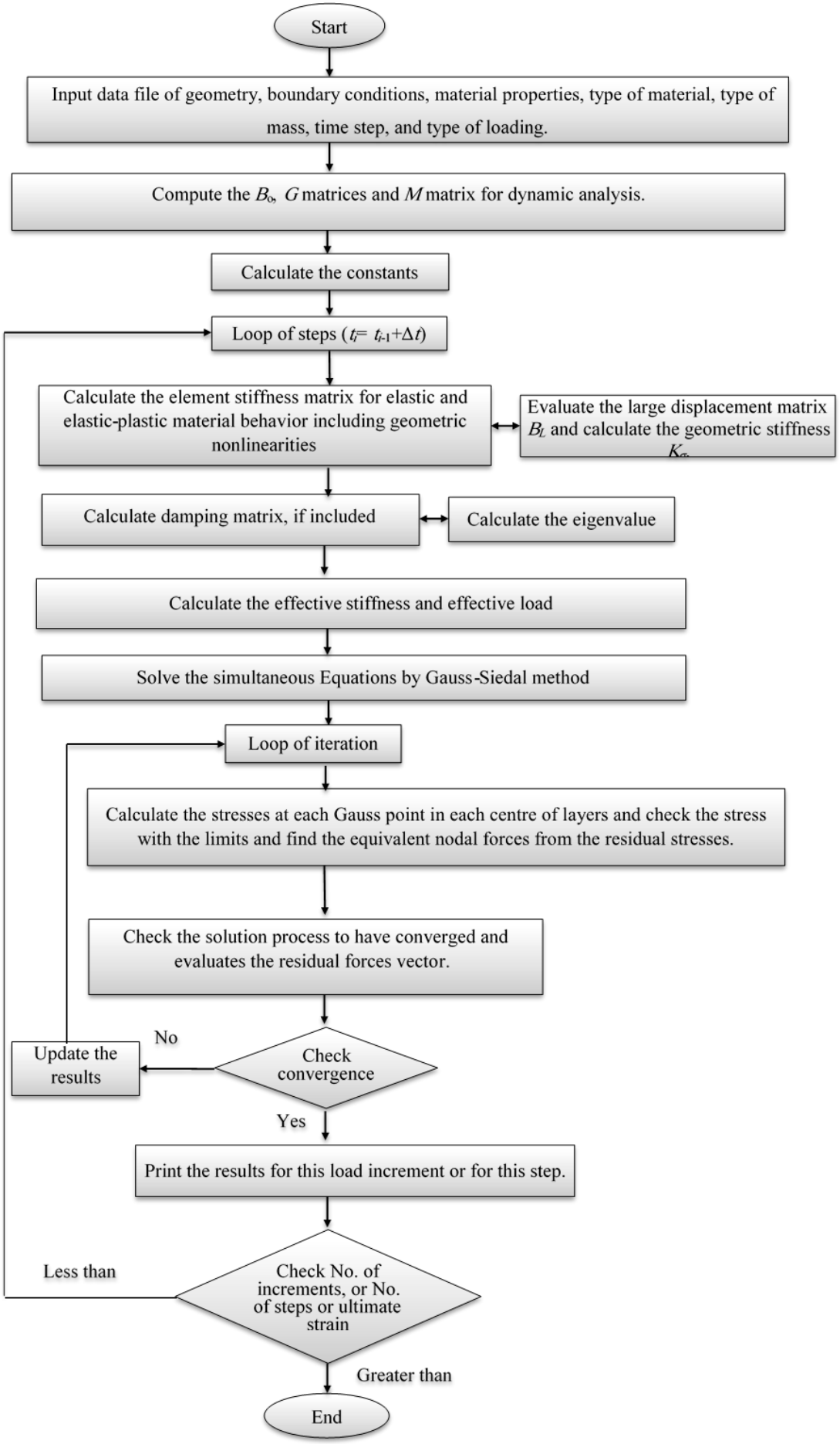

Figure 3. Dynamic analysis structure chart of computer program (FENSDAAP) [21]

5. Results and Discussion

5.1. Imperfect Laminated Composite Plate with Different Aspect Ratio

For studying the effectiveness of the variable fiber distribution and the orientation of the carbon fiber on the preformed dynamic non-linear behavior of the imperfect laminated composite plate with a different aspect ratio and SSSS boundary condition, the most important items drawn from the results should be understood:

- Results of $w_o/h= 0.00$ in Figure 4-a were considered the standard, and all results were compared against it.
- Figures 4 to 6 represent the elastic-plastic large deformation behavior of a laminated composite plate subjected to a constant uniform in-plane compressive load and are analyzed for different aspect ratios (1.0, 0.5, and 2.0) progressively with a varying magnitude of the initial imperfection from 0.0, 0.25, 0.5 to 1.0 for studying the effect of the variable carbon fiber distribution based on Equations 2-2 and 3-3 with the symmetrical orientation (0, 90, -90, 0) carbon fiber. The three figures are detailed to describe a case of fiber distribution with and without changing orientation, as shown below:

    A. Unified of fiber direction and fiber distribution.

    B. Unified direction of fiber with fiber distribution based on Equation 2-2.

    C. Symmetric (0, 90, 0, 90) of fibers direction and fiber distribution based on Equation 2-2

    D. Unified direction of fiber with fiber distribution based on Equation 3-3.

    E. Symmetric (0, 90, 0, 90) of fiber direction and fiber distribution based on Equation 3-3.

- The effect of the initial imperfection on the models was very clear and led to an increase in the response of the plate to deformation in a shorter period of time and a decrease in the dynamic stability of the plate.
- The results of all cases recorded that the maximum elastic displacement of the plate decreases with the increase of the initial deficiency, although it maintains the traditional behavior based on the exponential relationship between the initial imperfection and a speed response and an amount of deformation of the plate. The explanation for this is that the direction of the initial deformation was parallel to the direction of the applied load, so it acted as stiffness for the plate. It is similar to the behavior of the bent paper in its middle when trying to cause another deformation produced by a load parallel to the bend.
- Understand the effect of the variation of distribution and orientation of carbon fibers on aspect ratio in the results shown in Figures 5 and 6 for a rectangular plate subjected to a load in the direction of width (a) passed through, knowing the direction of carbon fiber spreading in the mass matrix and its relationship with other ruler parameters such as the load, effective length, boundary condition, etc. Where the fiber spreading in all models that weren't subjected to rotation was fixed in direction with the plate's width (a) made studying the effect of distribution and direction of fibers, loading direction, and aspect ratio at the same time was more accurate.
- The variable carbon fiber distribution in the unified and symmetrical orientations reduced the deficient laminated composite plate response to deformation significantly, and changing direction fibers enhanced this gain, as will be detailed with all aspect ratios analyzed in this study.

5.1.1. Aspect Ratio 1.0

Figures 4a to 4e show the following:

- Changing the fiber distribution according to Equations 2-2 and 3-3 without changing its direction in (B) and (D), respectively, reduced the distortion by half, noting that the dynamic stability of the distribution according to Equation 3-3 is better than Equation 2-2.
- The symmetrical rotation of the fibers in (C) and (E) with variable distribution in b and d respectively reduce the deformation up to 50% of its results in (Figure a) with high stability.
- Comparing the results of the displacement of the distribution of carbon fibers based on Equations 2-2 and 3-3 with the uniform and symmetrical direction gives preference to Equation 3-3.

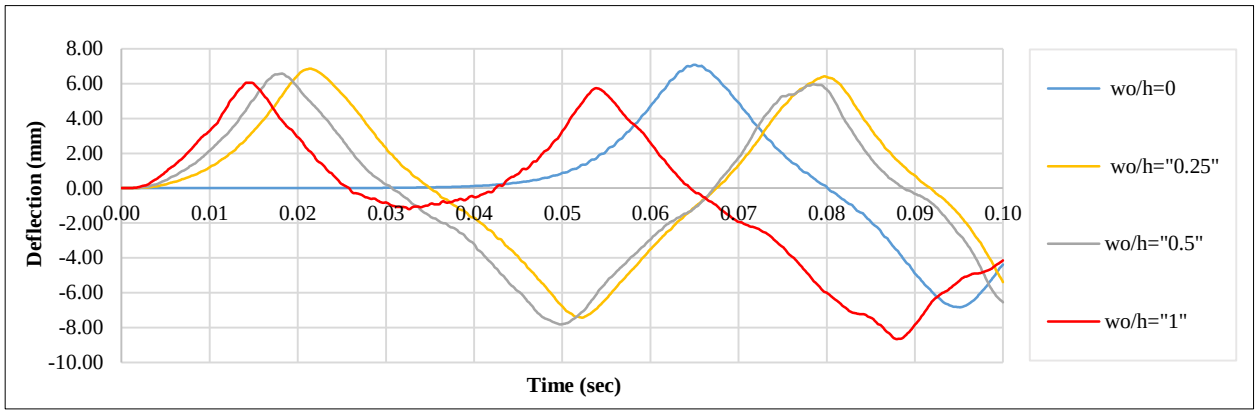

a) Unified orientation and distribution for carbon fiber of laminated composite plate with SSSS boundary condition

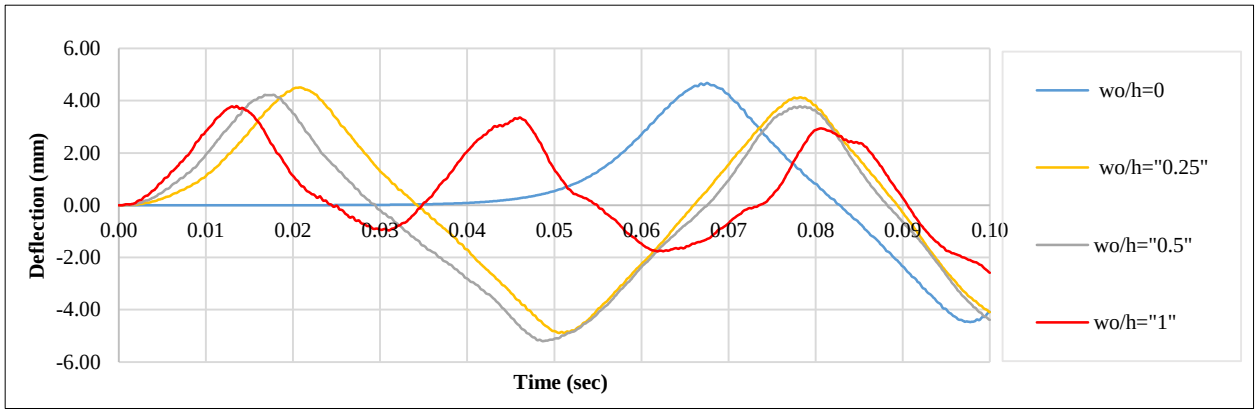

b) Unified orientation and a distribution based on Equation 2-2 for carbon fiber of laminated composite plate with SSSS boundary condition

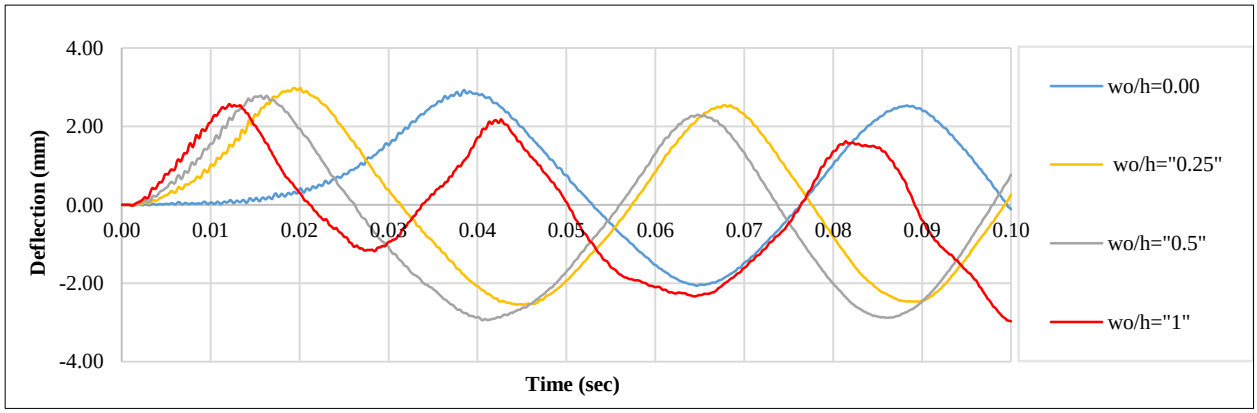

c) Symmetric orientation (0, 90, -90, 0) and a distribution based on Equation 2-2 for carbon fiber of laminated composite plate with SSSS boundary condition

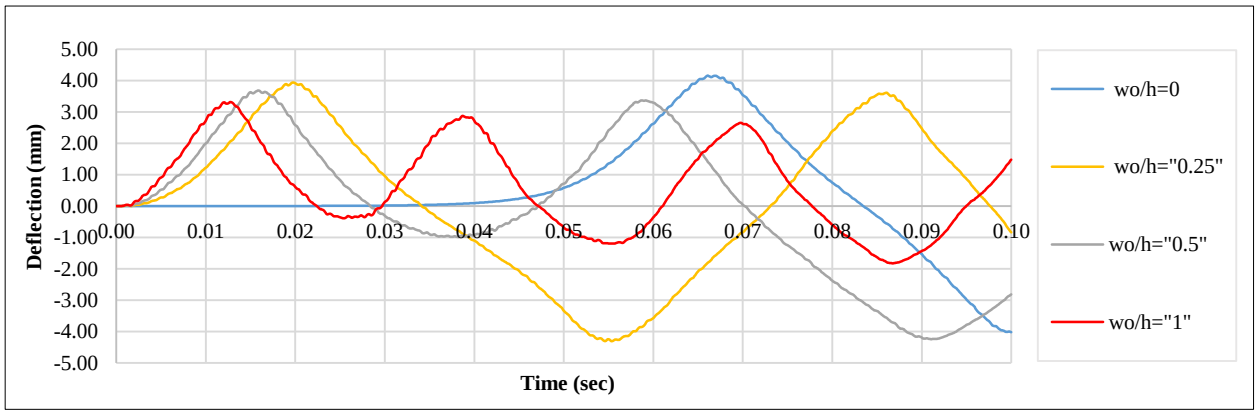

d) Unified orientation and a distribution based on Equation 3-3 for carbon fiber of laminated composite plate with SSSS boundary condition

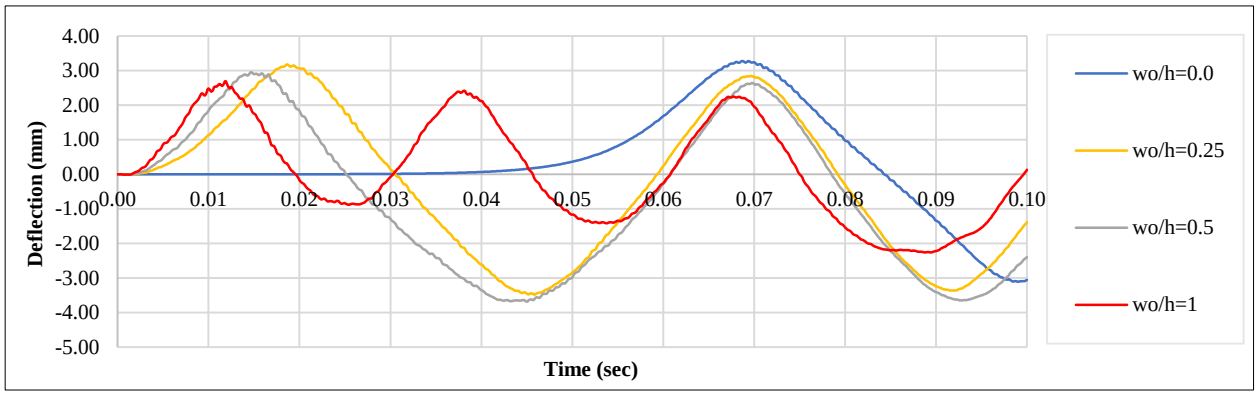

e) Symmetric orientation (0, 90, -90, 0) and a distribution based on Equation 3-3 for carbon fiber of laminated composite plate with SSSS boundary condition

Figure 4. Effectiveness of the initial imperfection on elastic-plastic displacement of the laminated composite plates with a different distribution and orientation of carbon fiber with SSSS boundary condition and 1.5 aspect ratio under an 800 KN uniform in-plane compression load in the X-axis direction at a time step (Δt) =0.0001 [sec].

5.1.2. Aspect Ratio (a/b) 0.5

The most significant unique properties resulting from the analysis of a laminated composite plate with an aspect ratio (a/b) = 0.5 are shown in Figures 5-a to 5-e, in addition to the basic explanations above:

- Based on comparing the results of Figure 5-a with Figure 4-a, it was extremely evident how reducing the aspect ratio from 1.0 to 0.5 had an impact on the dynamic behavior of the plate.
- Effected the results of this plate by the initial imperfection was significantly greater than its predecessors.
- Changing the distribution of carbon fibers reduced the negative effects of the initial imperfection and reduced the elastic displacement in Figure 5a to half the value as shown in Figures 5b and 5d, which gave a higher dynamic stability than the variable orientation models, which in turn gave a lower value of the large elastic-plastic displacement as shown in Figures 5c and 5e.

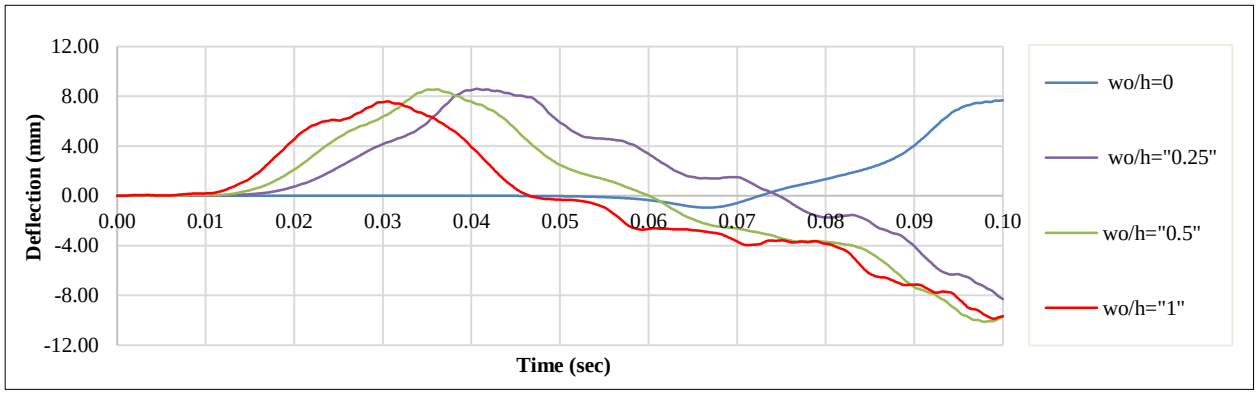

a) Unified orientation and distribution for carbon fiber of laminated composite plate with SSSS boundary condition

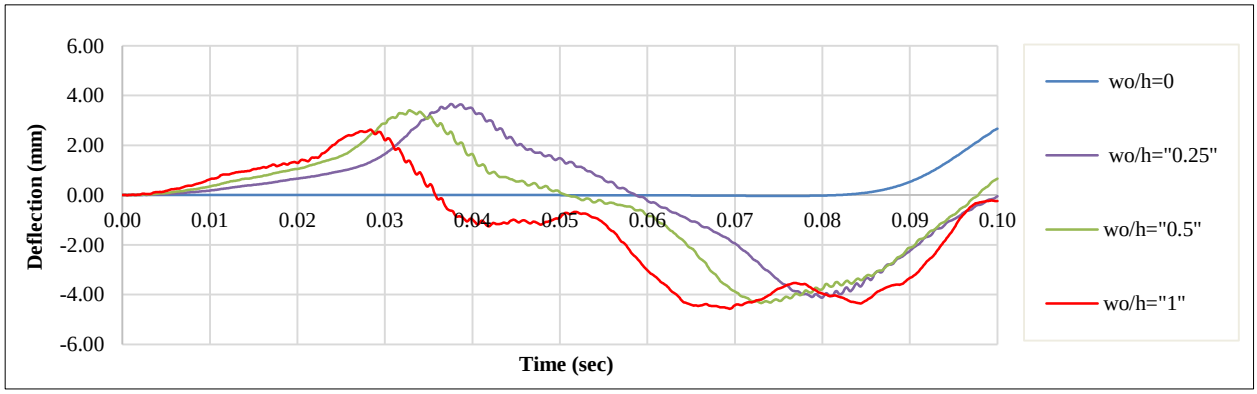

b) Unified orientation and a distribution based on equation 2-2 for carbon fiber of laminated composite plate with SSSS boundary condition

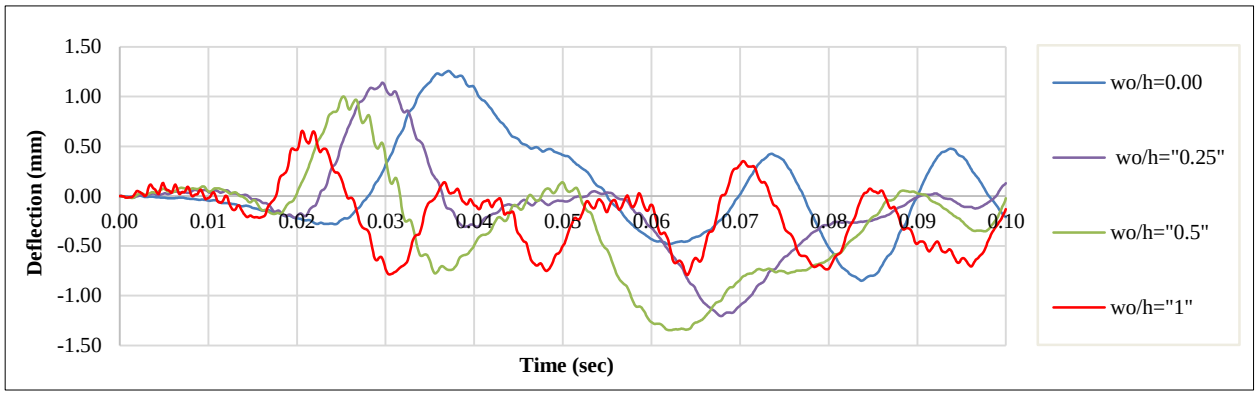

c) Symmetric orientation (0, 90, -90, 0) and a distribution based on equation 2-2 for carbon fiber of laminated composite plate with SSSS boundary condition

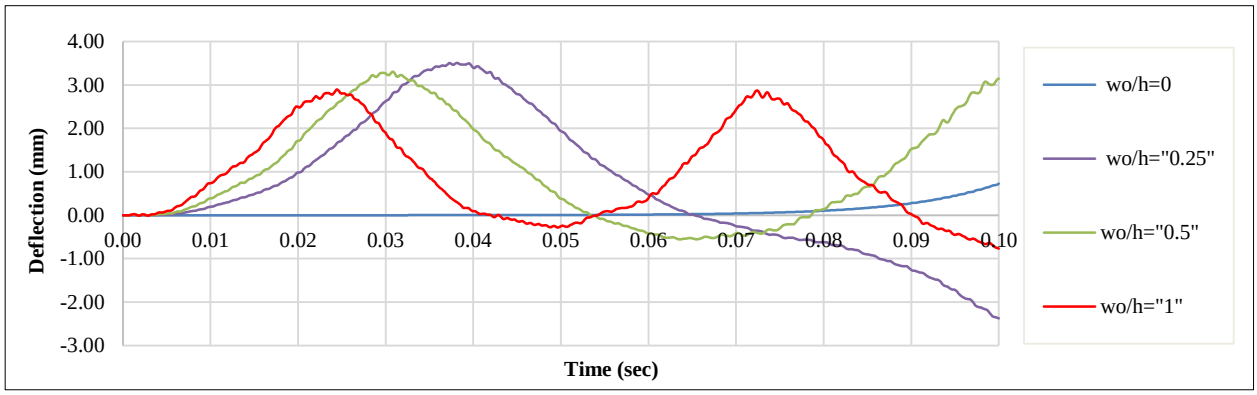

d) Unified orientation and a distribution based on equation 3-3 for carbon fiber of laminated composite plate with SSSS boundary

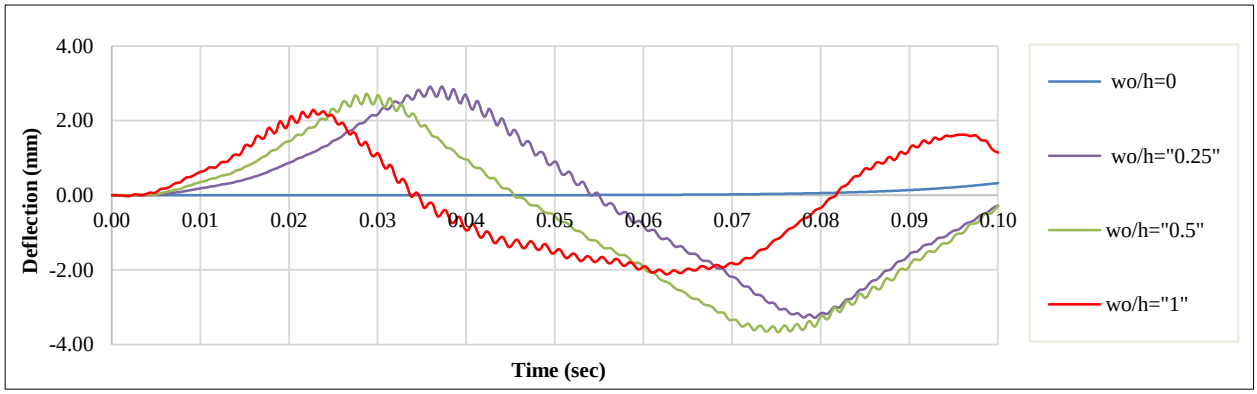

e) Symmetric orientation (0, 90, -90, 0) and a distribution based on equation 3-3 for carbon fiber of laminated composite plate with SSSS boundary condition

Figure 5. Effectiveness the initial imperfection on elastic-plastic displacement of the laminated composite plates with a different distribution and orientation of carbon fiber with SSSS boundary condition and 0.5 aspect ratio under 800 KN uniform in-plane compression load in X-axis direction at a time step *(Δt)* =0.0001[sec].

5.1.3. Aspect Ratio 2.0

Studying an aspect ratio represents studying the effect of changing the direction of the load from transverse to longitudinal at the same time, which contributed to obtaining significantly different results from those considered in paragraphs 5.1.1 and 5.1.2. As follows:

- Figure 6-a illustrates the effect of a longitudinal loading, which caused a significant destabilization of the plate's dynamic stability and greatly increased its deformation response, reaching approximately 1.5 of the deformation in Figure 4-a.
- Changing the distribution of fibers based on equation 2-2 was not efficient in reducing the plate's deformation response, as shown in Figure 6-b, while the distribution based on equation 3-3 was really very effective in reducing the sample's response to deformation (Figure 6-d).
- Both distributions 2-2 and 3-3 contributed to improving the dynamic stability of the board, and the first distribution was the best in this aspect.

- The symmetrical orientation of the distributed carbon fibers according to Equation 2-2 had a positive effect on improving the dynamic stability of the plate (Figure 6-C). While the symmetrical orientation of the distributed carbon fibers based on Equation 3-3 was very effective in reducing the plate's response to deformation in addition to improving its stability proportionally.

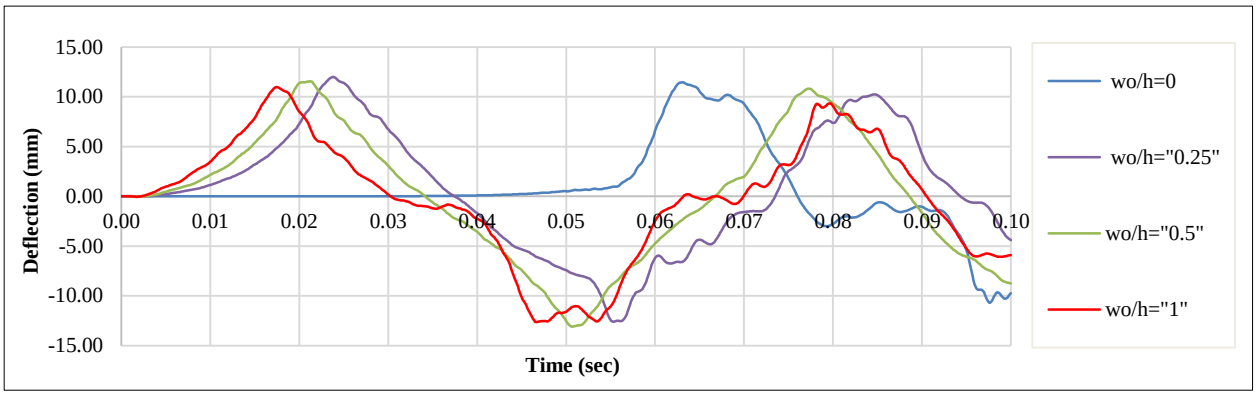

a) Unified orientation and distribution for carbon fiber of laminated composite plate with SSSS boundary condition

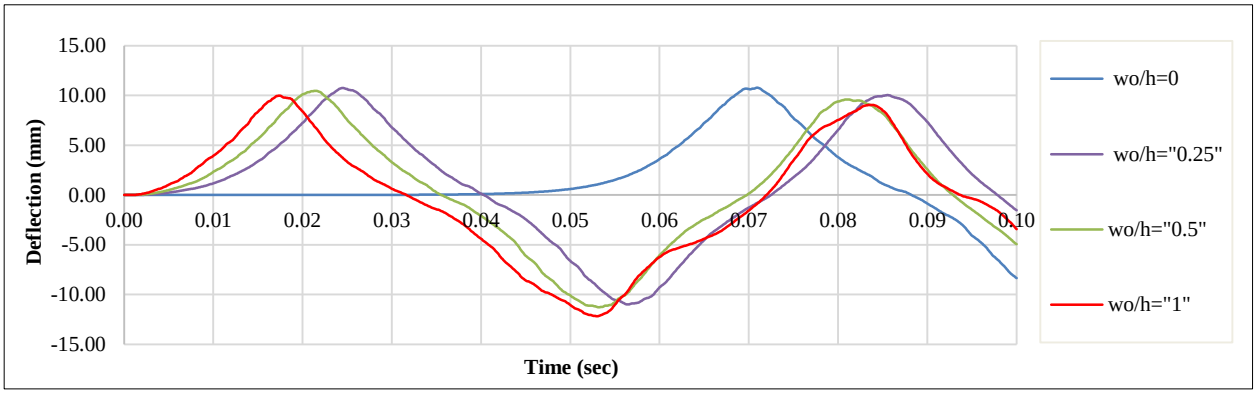

b) Unified orientation and a distribution based on equation 2-2 for carbon fiber of laminated composite plate with SSSS boundary condition

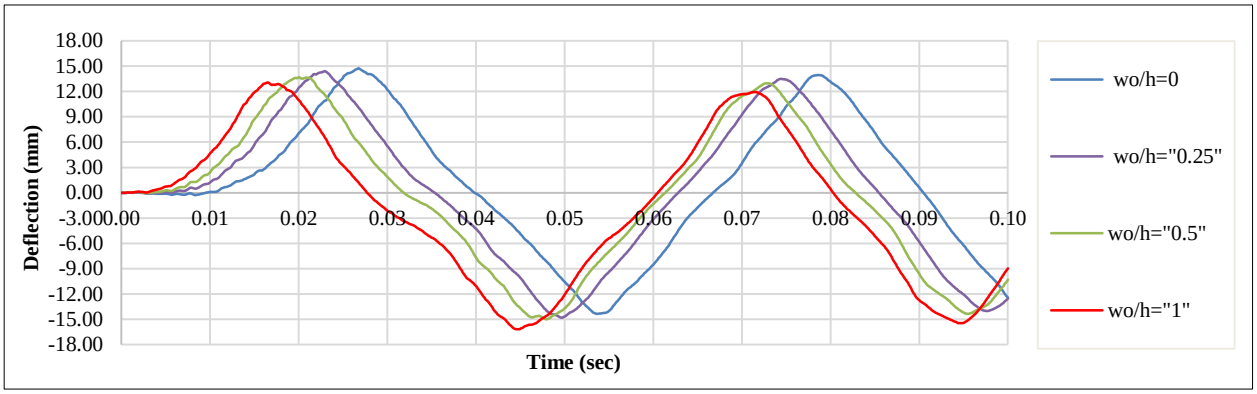

c) Symmetric orientation (0, 90, -90, 0) and a distribution based on equation 2-2 for carbon fiber of laminated composite plate with SSSS boundary condition

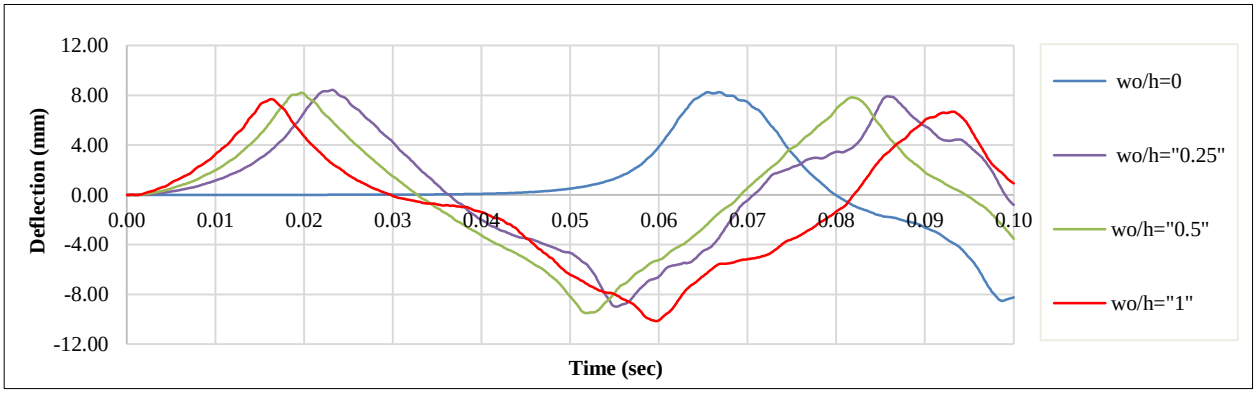

d) Unified orientation and a distribution based on equation 3-3 for carbon fiber of laminated composite plate with SSSS boundary condition

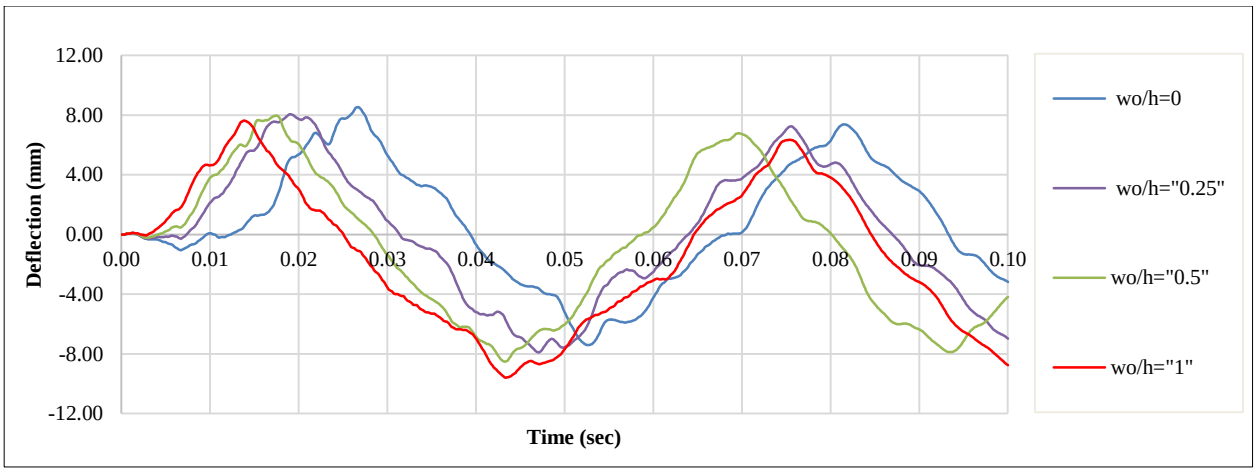

e) Symmetric orientation (0, 90, -90, 0) and a distribution based on equation 3-3 for carbon fiber of laminated composite plate with SSSS boundary condition

Figure 6. Effectiveness the initial imperfection on elastic-plastic displacement of the laminated composite plates with a different distribution and orientation of carbon fiber with SSSS boundary condition and 2.0 aspect ratio under 800 KN uniform in-plane compression load in X-axis direction at a time step *(Δt)* =0.0001[sec].

5.2. Imperfect Laminated Composite Plate with Different Bounder Condition

Effects of the laminated composite plate's deferential border condition and varied carbon fiber distribution and orientation on the plate's initial imperfections the plate from paragraph 5.1.1 is analyzed in the paragraphs to follow using various boundary conditions (SCSC and CCCC).

SSSS: A Boundary Condition when the All Edges of Plate is Simply Supported Articulated in the Section 5.1.1

CCCC: A Boundary Condition when All Edges of Plate is Clamped:

- Restricting of the plate edges completely did not prevent the appearance of the effect of the negative initial imperfection by increasing the sample's response to deformation and reducing its dynamic stability acquired from the engineering properties of this pattern of the boundary.
- Complete restriction of all edges of plate showed the Proportionality between the large elastic - plastic displacement and the value of the initial imperfection, confirming the exegesis given in Section 5-1 about the displacement values decrease with the increase in the initial decrease in the plate.
- Efficacy of differential distribution and orientation of the carbon fibers of the imperfect sheet. It is clear in Figures 7-b and 7-d.
- Fiber distribution based on equation 3-3 is best synchronized with symmetrical routing as shown in Figures 7-c and 7-e.

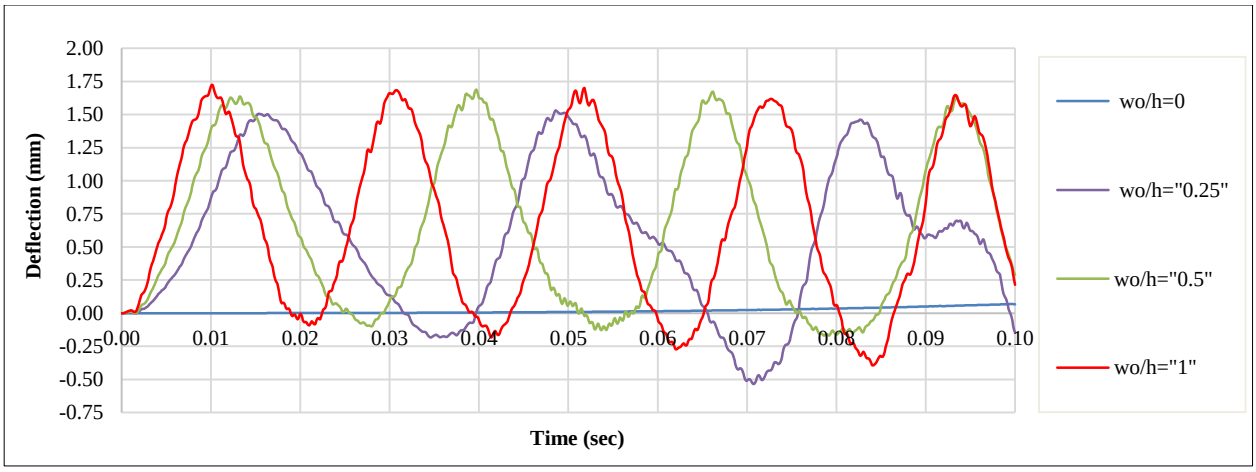

a) Unified orientation and distribution for carbon fiber of laminated composite plate with CCCC boundary condition

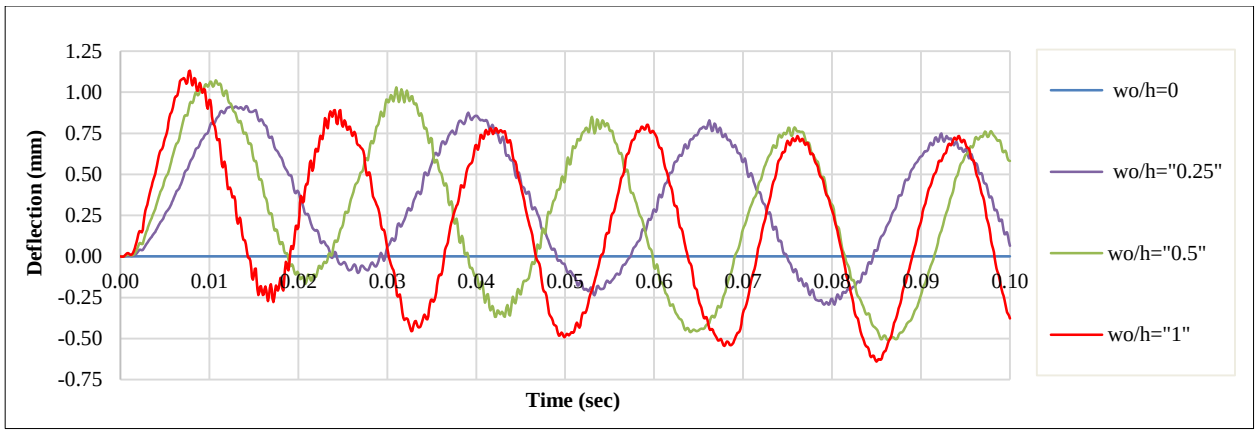

b) Unified orientation and a distribution based on equation 2-2 for carbon fiber of laminated composite plate with CCCC boundary condition

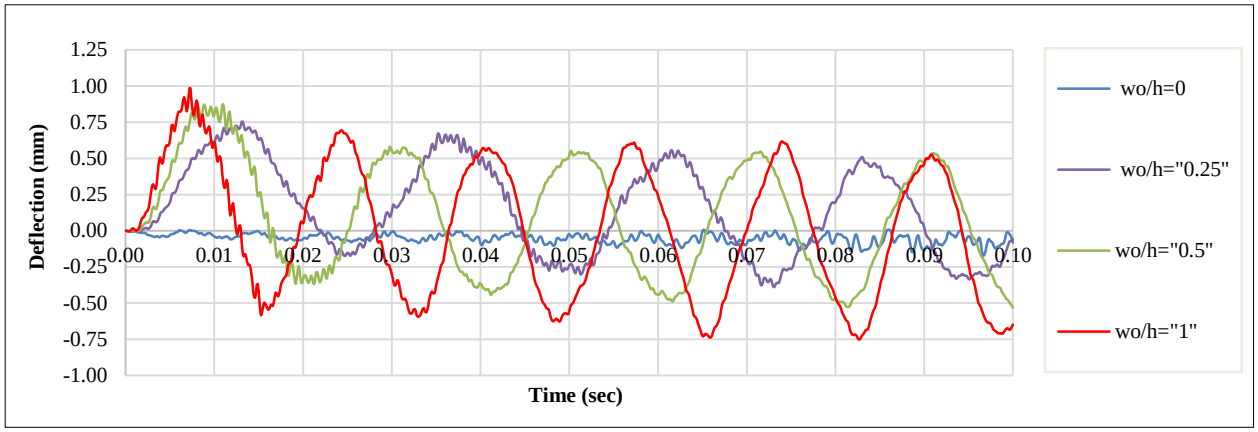

c) Symmetric orientation (0, 90, -90, 0) and a distribution based on equation 2-2 for carbon fiber of laminated composite plate with CCCC boundary condition

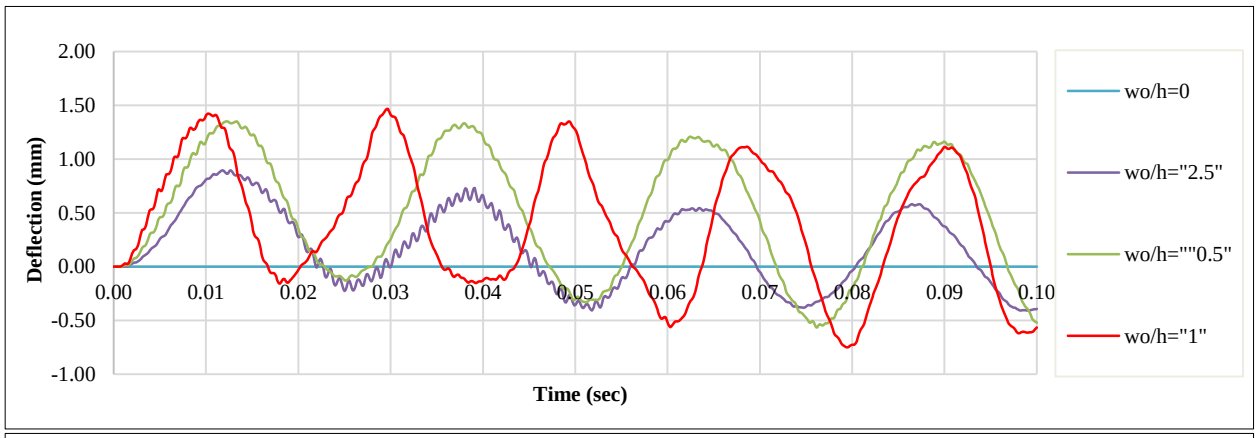

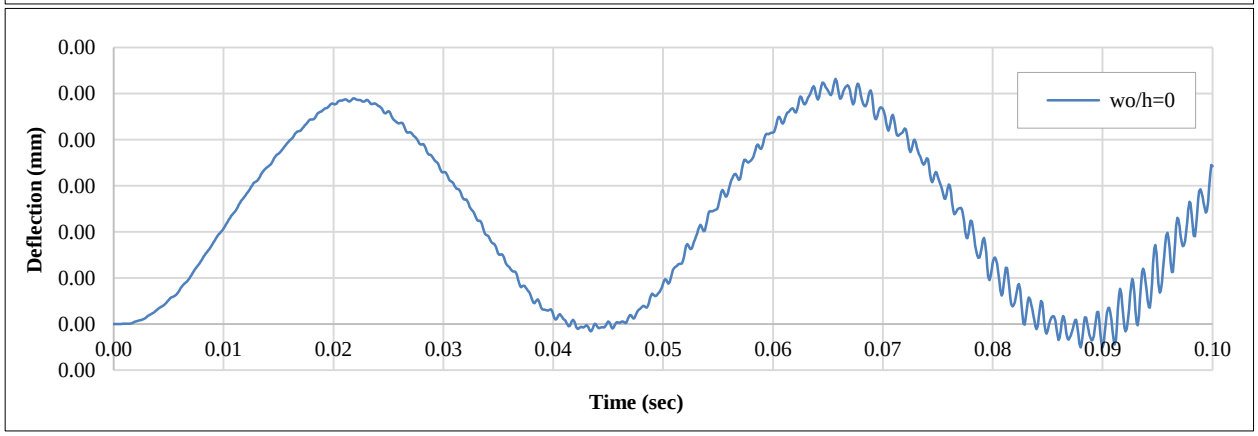

d) Unified orientation and a distribution based on equation 3-3 for carbon fiber of laminated composite plate with CCCC boundary condition

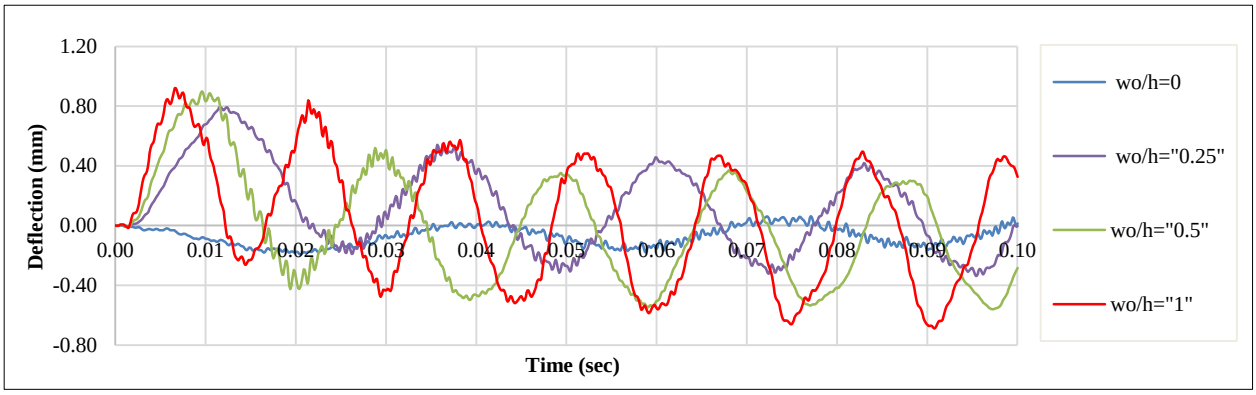

e) Symmetric orientation (0, 90, -90, 0) and a distribution based on equation 3-3 for carbon fiber of laminated composite plate with CCCC boundary condition

Figure 7. Effectiveness the initial imperfection on elastic-plastic displacement of the laminated composite plates with a different distribution and orientation of carbon fiber with CCCC boundary condition and 1.0 aspect ratio under 800 KN uniform in-plane compression load in X-axis direction at a time step *(Δt)* =0.0001[sec].

SCSC:

A boundary condition when a two edges of plate in load direction is clamped and another two edges of plate is simply supported

- The compound restriction studied in this paragraph is the complete restriction(fixed) of the two edges of the plate that are subject to the constant load in- plane and the boundary condition of the other two edges was simply support
- Figures 8-b and 8-d prove the reduced of response of the plate to deformation by changing the distribution pattern and the orientation of the carbon fibers of the laminated composite plate compared to Figure 8-a.
- The symmetrical orientation of the carbon fibers contributed to a reduction in elastic displacement with a slight decrease in dynamic stability, figures 8-c and 8-e.

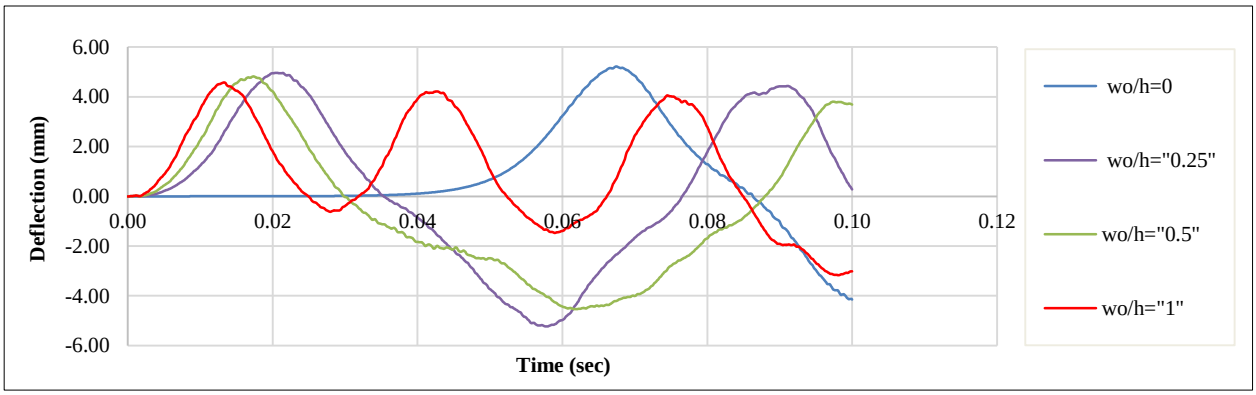

a) Unified orientation and distribution for carbon fiber of laminated composite plate with SCSC boundary condition

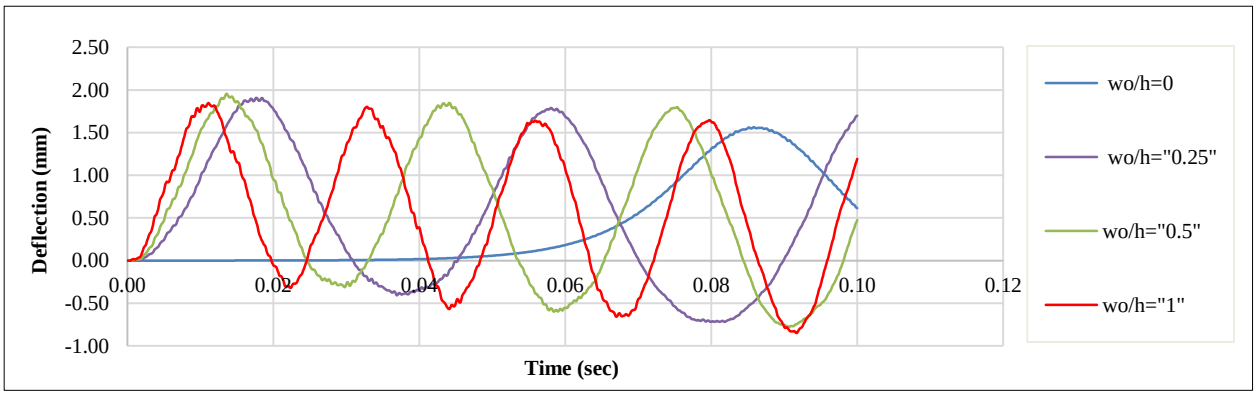

b) Unified orientation and a distribution based on equation 2-2 for carbon fiber of laminated composite plate with SCSC boundary condition

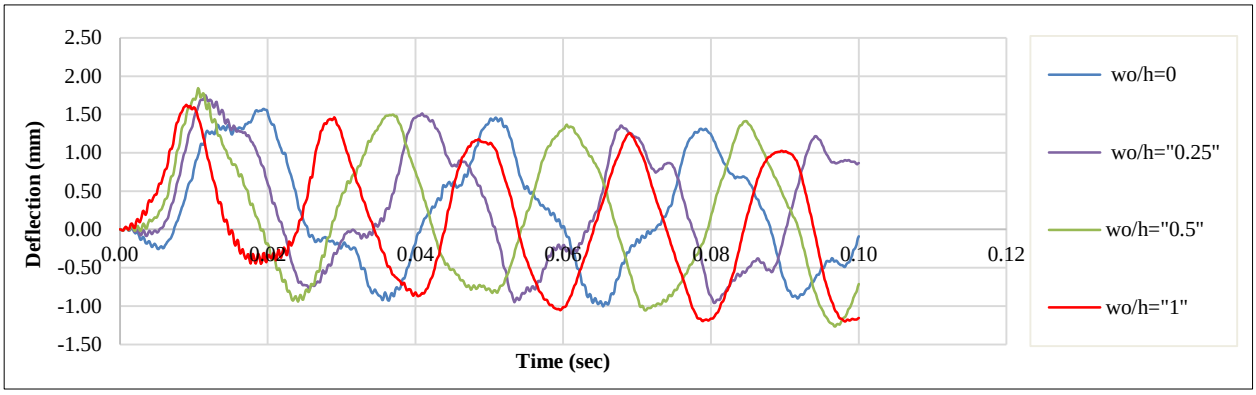

c) Symmetric orientation (0, 90, -90, 0) and a distribution based on equation 2-2 for carbon fiber of laminated composite plate with SCSC boundary condition

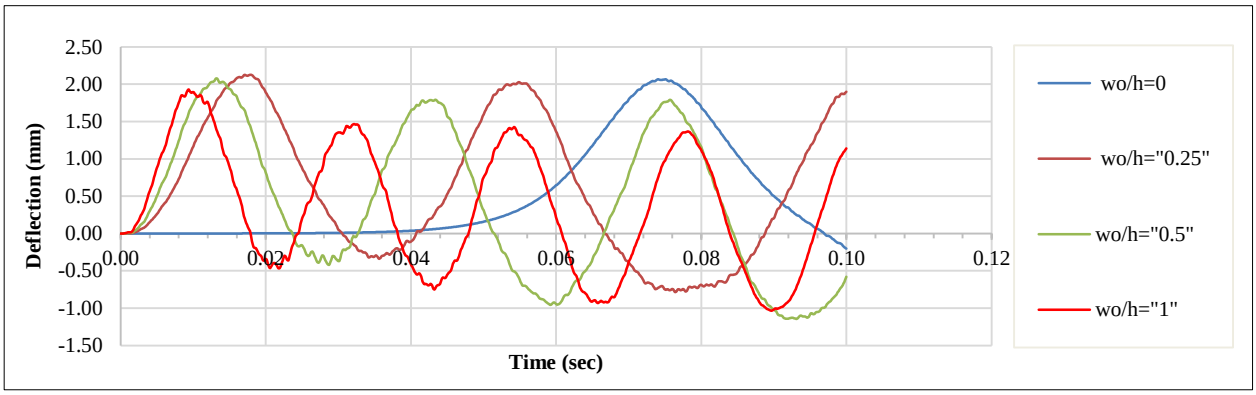

d) Unified orientation and a distribution based on equation 3-3 for carbon fiber of laminated composite plate with SCSC boundary condition

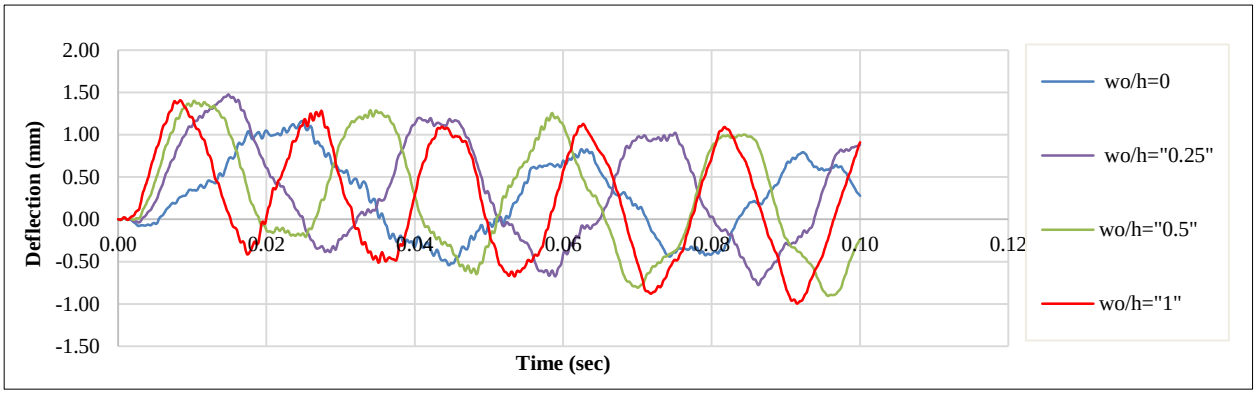

e) Symmetric orientation (0, 90, -90, 0) and a distribution based on equation 3-3 for carbon fiber of laminated composite plate with SCSC boundary condition

Figure 8. Effectiveness the initial imperfection on elastic-plastic displacement of the laminated composite plates with a different distribution and orientation of carbon fiber with SCSC boundary condition and 1.0 aspect ratio under 800 KN uniform in-plane compression load in X-axis direction at a time step *(Δt)* =0.0001[sec].

6. Conclusions

This study investigated the previous studies, proved that the effect of changing the geometric parameters in optimization the non-linear dynamic performance of laminated composite plate such as aspect ratio, and slenderness ratio, is more effective than improving the infrastructure, but in the same time, it has proved the investment efficiency in the optimization of the infrastructure orthogonal performance characteristics of laminated composite plate in improving dynamic performance, this approach has given more freedom to designers and manufacturers of this type of plates for finding solving to initial imperfection, holes, reduced the plats response to deformation and increasing the buckling strength without resorting to geometric parameters.

This study showed the possibility of reducing the side effects of the initial imperfection by using the fiber carbon distribution based on the Equations 2-2 and 3-3 from Leissa and Martine's equations. In all the analyzed models, the symmetrical orientation was effective in reducing the imperfect composite plate's response to deformation and relatively reducing its dynamic stability, which gave a clear indication of the effectiveness of the relationship between the load

direction and the carbon fiber deployment direction on the plate's stability and stiffness. Recommendations: The high sensitivity of the laminated composite plate optimizations based on changing the distribution and direction of the carbon fibers proven in this study obliges those interested in its manufacture and use to do the following:

- Knowing the impact of the characteristics of the load (a pattern, a direction, a position (in or out of plane), etc.), the properties of the boundary condition, and the geometric characteristics of the plate (thickness, slenderness ratio, aspect ratio, initial imperfection, geometrical properties of openings, temperatures, etc.) on the optimization of the structural properties of the plate (Number of layers, fiber distribution style, fiber direction style, fiber percentage in the mass matrix, etc.).
- Study the effect of the above influences on each other before studying the effect of improvements on them to distinguish the effect of all those parameters separately for choosing the optimal method to improve the dynamic performance and reduce panel response to deformation.

7. Declarations

7.1. Author Contributions

Conceptualization, W.M. and H.A.; methodology, S.S.; software, W.M.; validation, W.M., SS., and H.A.; formal analysis, W.M.; investigation, W.M.; resources, S.S.; data curation, W.M.; writing—original draft preparation, W.M.; writing—review and editing, S.S.; visualization, W.H. and S.S.; supervision, S.S. and H.A.; project administration, W.M. and H.A.; funding acquisition, W.M. All authors have read and agreed to the published version of the manuscript.

7.2. Data Availability Statement

The data presented in this study are available in the article.

7.3. Funding

The authors received no financial support for the research, authorship, and/or publication of this article.

7.4. Conflicts of Interest

The authors declare no conflict of interest.

8. References

[1] Ferreira, R. T. L., & Ashcroft, I. A. (2020). Optimal orientation of fiber composites for strength based on Hashin's criteria optimality conditions. Structural and Multidisciplinary Optimization, 61(5), 2155–2176. doi:10.1007/s00158-019-02462-w.

[2] Tsai, S. W., & Wu, E. M. (1971). A General Theory of Strength for Anisotropic Materials. Journal of Composite Materials, 5(1), 58–80. doi:10.1177/002199837100500106.

[3] Toyoda, M. (1991). Strength characteristics of composite materials. Welding International, 5(5), 341–345. doi:10.1080/09507119109446748.

[4] Kondratiev, A. V., Gaidachuk, V. E., & Kharchenko, M. E. (2019). Relationships between the ultimate strengths of polymer composites in static bending, compression, and tension. Mechanics of Composite Materials, 55, 259-266. doi:10.1007/s11029-019-09808-x.

[5] Azzi, V. D., & Tsai, S. W. (1965). Anisotropic strength of composites - Investigation aimed at developing a theory applicable to laminated as well as unidirectional composites, employing simple material properties derived from unidirectional specimens alone. Experimental Mechanics, 5(9), 283–288. doi:10.1007/BF02326292.

[6] Joshi, R., & Pal, P. (2021). Ply-by-ply failure analysis of laminates under dynamic loading. Sound and Vibration, 55(2), 173–190. doi:10.32604/SV.2021.011387.

[7] Adams, R. D., & Bacon, D. G. C. (1973). Effect of Fiber Orientation and Laminate Geometry on the Dynamic Properties of CFRP. Journal of Composite Materials, 7(4), 402–428. doi:10.1177/002199837300700401.

[8] Leissa, A. W., & Martin, A. F. (1990). Vibration and buckling of rectangular composite plates with variable fiber spacing. Composite Structures, 14(4), 339–357. doi:10.1016/0263-8223(90)90014-6.

[9] Pandey, M. D. (1999). Effect of fiber waviness on buckling strength of composite plates. Journal of engineering mechanics, 125(10), 1173-1179. doi:10.1061/(ASCE)0733-9399(1999)125:10(1173).

[10] Williams, D. G., & Walker, A. C. (1975). Explicit Solutions for the Design of Initially Deformed Plates Subject to Compression. Proceedings of the Institution of Civil Engineers, 59(4), 763–787. doi:10.1680/iicep.1975.3638.

[11] Yang, J., Liew, K. M., & Kitipornchai, S. (2006). Imperfection sensitivity of the post-buckling behavior of higher-order shear deformable functionally graded plates. International Journal of Solids and Structures, 43(17), 5247–5266. doi:10.1016/j.ijsolstr.2005.06.061.

[12] Feddal, I., Khamlichi, A., & Ameziane, K. (2018). Effects of plies orientations and initial geometric imperfections on buckling strength of a composite stiffened panel. MATEC Web of Conferences, 191, 8–11. doi:10.1051/matecconf/201819100008.

[13] Ghannadpour, S. A. M., & Mehrparvar, M. (2020). Modeling and evaluation of rectangular hole effect on nonlinear behavior of imperfect composite plates by an effective simulation technique. Composite Materials and Engineering, 2(1), 25–41. doi:10.12989/cme.2020.2.1.025.

[14] Al-Ramahee, M. A., & Abodi, J. T. (2020). Effect of variable fiber spacing on dynamic behavior of a laminated composite plate. Journal of Green Engineering, 10(11), 12663–12677.

[15] Mondal, S., & Ramachandra, L. S. (2020). Nonlinear dynamic pulse buckling of imperfect laminated composite plate with delamination. International Journal of Solids and Structures, 198, 170–182. doi:10.1016/j.ijsolstr.2020.04.010.

[16] Cetkovic, M. (2022). Influence of initial geometrical imperfections on thermal stability of laminated composite plates using layerwise finite element. Composite Structures, 291, 115547. doi:10.1016/j.compstruct.2022.115547.

[17] Thor, M., Mandel, U., Nagler, M., Maier, F., Tauchner, J., Sause, M. G. R., & Hinterhölzl, R. M. (2021). Numerical and experimental investigation of out-of-plane fiber waviness on the mechanical properties of composite materials. International Journal of Material Forming, 14(1), 19–37. doi:10.1007/s12289-020-01540-5.

[18] Barbero, E. J., & Reddy, J. N. (1991). Modeling of delamination in composite laminates using a layer-wise plate theory. International Journal of Solids and Structures, 28(3), 373–388. doi:10.1016/0020-7683(91)90200-Y.

[19] Nguyen-Xuan, H., Thai, C. H., Bleyer, J., & Nguyen, P. V. (2014). Upper bound limit analysis of plates using a rotation-free isogeometric approach. Asia Pacific Journal on Computational Engineering, 1(1). doi:10.1186/s40540-014-0012-5.

[20] Ammash, H. (2008). Nonlinear Static and Dynamic Analysis of Laminated Plates Under In-plane Forces Some of the authors of this publication are also working on these related projects: Stability in Elastic-plastic States of Columns View project Stability of Plates and Shells View project (Issue November). doi:10.13140/RG.2.2.33369.01128.

[21] Mohammed, W. H., Shambina, S., & Ammash, H. K. (2022). Effect of Fibers Orientation on the Nonlinear Dynamic Performance of Laminated Composite Plate under Different Loading In-plane. Civil Engineering Journal, 8(12), 2706–2720. doi:10.28991/CEJ-2022-08-12-03.